

The Optical Properties of the Bc₂DDQ Crystal and Its Solid Phase Reaction

Masashi TANAKA,* Shizuaki MURATA, Hideo TAKEUCHI,†
and Susumu MATSUO†

Department of Chemistry, College of General Education, Nagoya University, Chikusa-ku, Nagoya 464-01

†Department of Physics, College of General Education, Nagoya University, Chikusa-ku, Nagoya 464-01

(Received March 2, 1992)

Benzo[*c*]cinnoline (Bc) and 2,3-dichloro-5,6-dicyano-1,4-benzoquinone (DDQ) give a charge-transfer (CT) complex with the formula Bc₂DDQ. The reflection spectra of the crystal of the Bc₂DDQ complex were measured and the charge-transfer degree in the Bc₂DDQ complex was estimated to be about 18%. This crystal exhibits a solid-phase reaction at 138 °C. Its thermal reaction was studied by the differential scanning calorimetry, thermogravimetry and the GC/MS spectra as well as the IR and ESR spectra and the temperature dependence of the magnetic susceptibility.

It is well known that *p*-benzoquinone and its derivatives react with various electron donors via CT complexes.¹⁾ One recent example was reported by Osawa et al.,²⁾ in which *p*-benzoquinones react with Wurster's Blue perchlorate upon being heated to give quinone dimers through CT complexes in an acetone solution. In the present paper we report on the optical properties and the solid-phase reaction of the crystalline CT complex of Bc₂DDQ. The thermochromism by the solid phase reaction of the CT complex has possible applications to molecular devices, like a compact disk-write once read many memory (CD-WORM).

Experimental

Red crystals of the Bc₂DDQ complex were obtained by slow evaporation of the solvent from a solution of commercial Bc (C₁₂H₈N₂) and DDQ (C₈Cl₂N₂O₂) (2:1 ratio) in ethyl acetate. The thermal reaction of Bc₂DDQ occurred upon heating at 160 °C for 40 h in air.

Thermal analyses were carried out using a Shimadzu DSC-50, a TGA-50 and a GC/MS at a heating rate of 10 °C min⁻¹ under N₂ or He gas. The IR spectra were recorded using a JASCO FTIR-7300 as the KBr disc; the UV-vis spectra were measured on a Hitachi-330 spectrophotometer. The reflection spectra of the Bc₂DDQ crystal were taken using a reflection spectrophotometer made in our laboratory;³⁾ the ESR spectra were also measured using equipment made in our laboratory. The magnetic susceptibility was measured using an Oxford magnetic balance.

Results and Discussion

Electronic Structure of Bc and DDQ Molecules.

The absorption spectra of Bc and DDQ at room temperature are given in Fig. 1. The first absorption bands were assigned to the *n*→*π** band, located at 25000 cm⁻¹ (*ε*=280 l mol⁻¹ cm⁻¹) for Bc⁴⁾ and 27000 cm⁻¹ (*ε*=760 l mol⁻¹ cm⁻¹) for DDQ,⁵⁾ respectively. The electronic structure of Bc and DDQ can therefore be depicted as shown in Fig. 2. Figure 2 shows an electronic configuration diagram obtained by an ab initio calculation of the SCF with the Gaussian 90 program and STO-3G basis

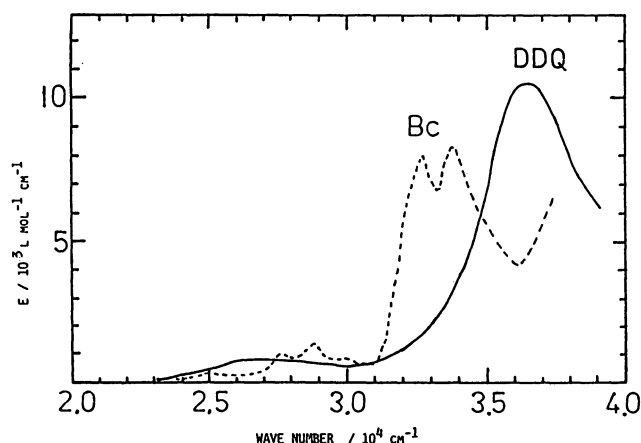


Fig. 1. Absorption spectra at room temperature of Bc (---) and DDQ (—) in ethyl acetate.

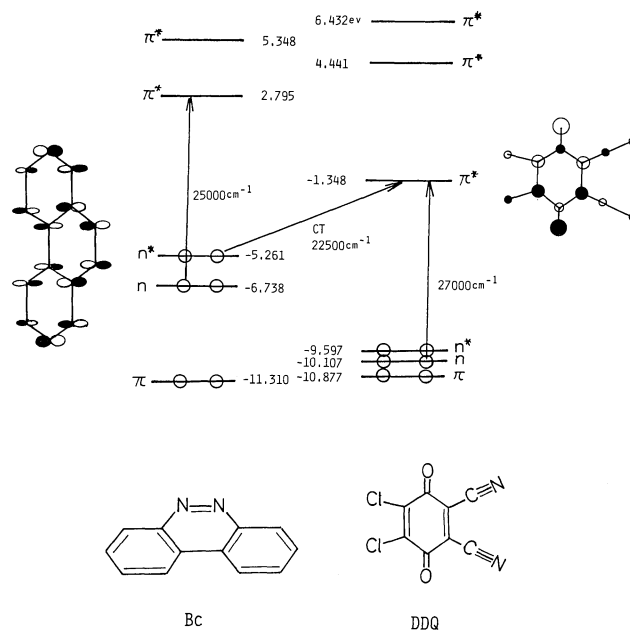


Fig. 2. Electronic structure of Bc and DDQ molecules.

set. The highest occupied molecular orbitals (HOMO) of Bc contains the n orbital on the nitrogen atoms; the lowest unoccupied molecular orbital (LUMO) of DDQ has the character of a π^* orbital.

Electronic Structure of the Bc₂DDQ Crystal. The crystal of Bc₂DDQ complex has two donors (Bc) and one acceptor (DDQ) in the asymmetric unit and a unique packing mode, as shown in Fig. 3.⁶⁾ The mean planes of adjacent donor and acceptor molecules are mutually nearly perpendicular. Both Bc's form short contacts with the central part of DDQ via their N–N bridges, which appear to have their lone pair lobes pointing at the π system of the acceptor. That is, the packing arrangement seems to have the maximum overlap between the HOMO (n^* orbital) of Bc and the LUMO (π^* orbital) of DDQ.

The reflection spectra of the crystal of the Bc₂DDQ complex were recorded in the 10000–35000 cm^{-1} range, as is shown in Fig. 4. The absorption spectra shown in Fig. 5 were obtained by a Kramers–Kronig analysis of the reflection spectra;³⁾ the maximum peak appears at about 24000 cm^{-1} ($\epsilon=3\times 10^4 \text{ l mol}^{-1} \text{ cm}^{-1}$). This band can be assigned to the $n^*\rightarrow\pi^*$ charge-transfer transition from the N lone pairs of Bc to the π^* orbital of DDQ.

The dielectric function of the Bc₂DDQ crystal can be expressed by the following equation;³⁾

$$\epsilon(\omega) = \epsilon_{\text{core}} + \sum_j \frac{\Omega_j^2}{\omega_j^2 - \omega^2 - i\omega\gamma_j}, \quad (1)$$

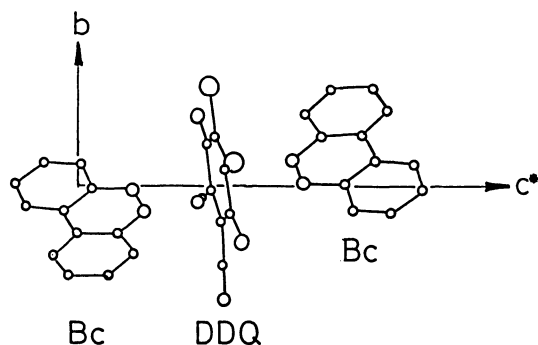


Fig. 3. View of the Bc₂DDQ crystal.⁶⁾

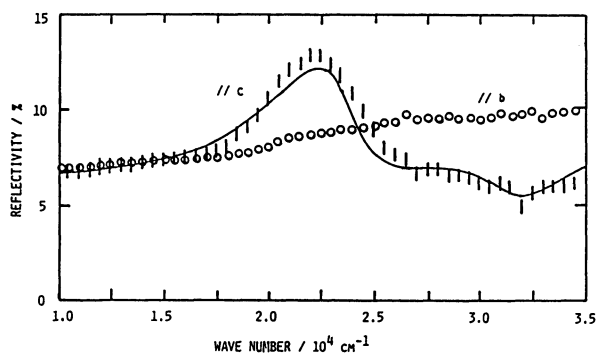


Fig. 4. Reflection spectra of the crystal of the Bc₂DDQ complex together with the best-fitted curve.

where $\Omega_j = (4\pi N e^2 f_j / m)^{1/2}$; $\hbar\omega_j$ and γ_j are the transition energy and the band width of the j -th band, respectively. $N=14.6\times 10^{20} \text{ cm}^{-3}$ is the number density of the Bc₂DDQ complex in the crystal, f_j is the oscillator strength of the j -th band and m is the electron mass.

The reflectivity (R) can be expressed using the dielectric function of Eq. 1,³⁾

$$R = \frac{1 + |\epsilon| - \sqrt{2(|\epsilon| + \epsilon_1)}}{1 + |\epsilon| + \sqrt{2(|\epsilon| + \epsilon_1)}}, \quad (2)$$

where $|\epsilon| = \sqrt{\epsilon_1^2 + \epsilon_2^2}$; ϵ_1 and ϵ_2 are the real and imaginary parts of the dielectric function, respectively. The parameters Ω_j , ω_j , and γ_j can be determined by a best fit of the calculated reflection values of the observed spectra. The obtained parameters are given in Table 1, and the best-fit curve is plotted in Fig. 4 together with the measured reflection spectra.

The Bc₂DDQ complex forms the configuration of the donor–acceptor alternative stacking (DAD) type in the crystal. The ground state can thus be described by the following wave function:^{7,8)}

$$\Psi_0 \cong \Phi(\text{DAD}) + \frac{b}{\sqrt{2}} \{ \Phi(\text{DA}^-\text{D}^+) + \Phi(\text{D}^+\text{A}^-\text{D}) \}, \quad (3)$$

Here, $\Phi(\text{DAD})$ represents a nonbonding ground state; $\Phi(\text{DA}^-\text{D}^+)$ and $\Phi(\text{D}^+\text{A}^-\text{D})$ are the CT transition state from the n^* orbital (D: Bc) to the acceptor (A: DDQ). The wave function $\Psi_{\text{CT}}(-)$ for the optically allowed CT band is given by

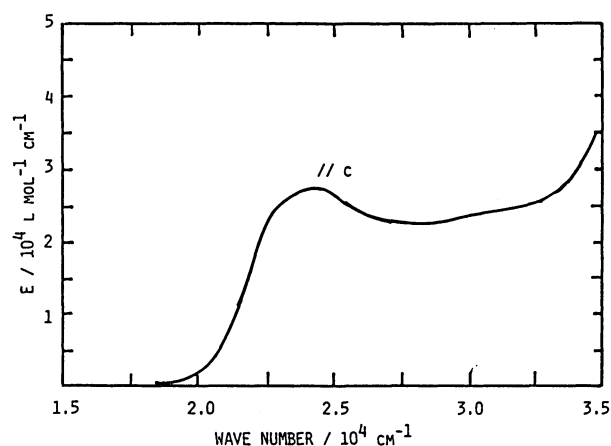


Fig. 5. C-axis absorption spectrum obtained by a K–K analysis of the reflection spectrum of the Bc₂DDQ crystal.

Table 1. Best Fitted Parameters of the Dielectric Function of the Bc₂DDQ Crystal

j	ω_j/cm^{-1}	Ω_j/cm^{-1}	γ_j/cm^{-1}	f_j
1	23000	12500	4000	1.2
2	27500	12000	8000	1.1
3	30000	9000	5000	0.6
4	35000	14000	5000	1.5

$\epsilon_{\text{core}}=2.0$.

$$\Psi_{CT}(-) = \frac{1}{\sqrt{2}} \{ \Phi(DA^-D^+) - \Phi(D^+A^-D) \}, \quad (4)$$

and the oscillator strength is defined theoretically as

$$f = 3 \times 1.085 \times 10^{11} \times \tilde{\nu}_{CT} b^2 |R_{AD}|^2. \quad (5)$$

Here, R_{AD} is the distance between the acceptor and the donor molecules in units of cm and $\tilde{\nu}_{CT}$ is the excitation energy in units of cm^{-1} .

The observed oscillator strength of the CT band ($j=1$) of the Bc₂DDQ crystal is $f=1.2$, as is shown in Table 1. The distance between Bc and DDQ is $R_{AD}=3 \times 10^{-8}$ cm and the excitation energy is $\tilde{\nu}_{CT}=23000$ cm^{-1} . The charge-transfer degree was thus calculated to be $b^2=0.18$. Such a charge-transfer effect is also observed

Table 2. IR Bands (cm^{-1}) of DDQ, Bc, and Bc₂DDQ Compounds

$\tilde{\nu}_0/\text{cm}^{-1}$		$\tilde{\nu}/\text{cm}^{-1}$	$\Delta\tilde{\nu}=\tilde{\nu}-\tilde{\nu}_0$
DDQ	Bc	Bc ₂ DDQ	
1674		1695	21
1550		1570	20
	1576	1550	26
	1431	1460	29
	1354	1360	6
1268		1265	-3
1173		1175	2
	1173	1170	-3
	1120	1140	20
802		795	-7
	760	765	5
	713	705	-8

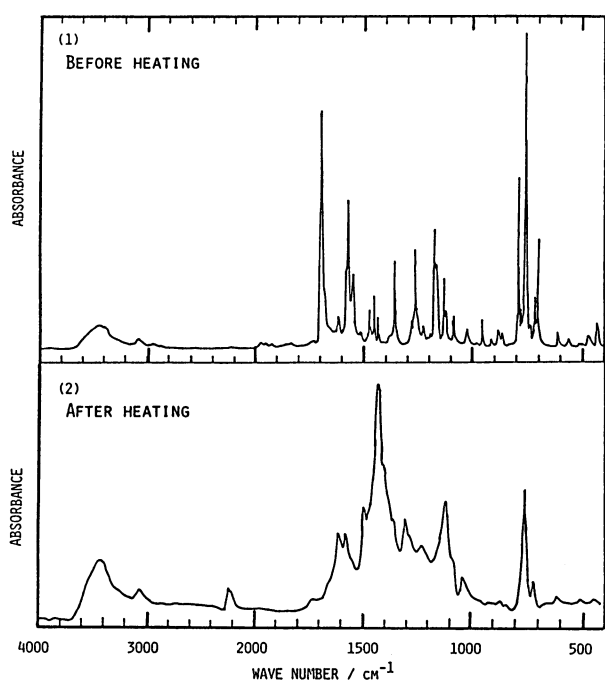


Fig. 6. IR spectra of the Bc₂DDQ complex before and after heating.

in the IR vibrational spectra, as is shown in Fig. 6 and Table 2. Many vibrational bands shift to a higher energy upon forming the CT complex, except for a few bands. Furthermore, the large charge-transfer degree contributes to the stabilization energy of the singlet ground state, making the Bc₂DDQ crystal antimagnetic. This is supported by the fact that there is no ESR signal of the Bc₂DDQ crystal.

Solid Phase Reaction of the Bc₂DDQ Complex.

Figure 7 shows the differential scanning calorimetry (DSC) and thermogravimetry (TG) curves of the Bc₂DDQ crystal. Upon heating, two endothermic peaks (138.1 and 241.3 °C) and an exothermic peak (258.5 °C) were observed for the DSC spectrum. The endothermic peak at 138.1 °C showed no weight change under TG analysis. The red crystal of Bc₂DDQ, however, changed to an insoluble black product upon being heated at temperature higher than 138 °C. Furthermore, the endothermic peak which appeared at 138.1 °C upon heating gave no corresponding peak upon cooling. It is thus suggested that an irreversible solid-phase reaction takes place at 138.1 °C. On the other hand, the endothermic peak which appears at 241.3 °C corresponds to the fusion of the black product and the exothermic peak at 258.5 °C is attributed to decomposition.

Fig. 8-(A) shows a mass chromatogram (MC) of the Bc₂DDQ crystal at a heating rate of 20 °C min⁻¹ under He gas; Figs. 8-(B) and (C) depict the mass spectra at 260 °C of the Bc₂DDQ crystal (B) and the Bc molecule (C). However, the mass spectra of the Bc₂DDQ crystal at 150 °C showed no peak. This fact corresponds to no weight change during a TG analysis at 150 °C. The peaks of the mass chromatogram at 260 °C may be interpreted in terms of evaporation of the Bc molecules.

The IR spectrum of the black product obtained upon

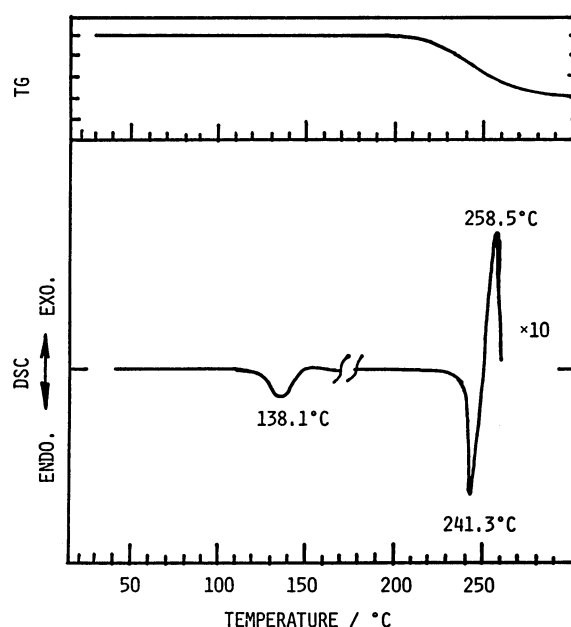
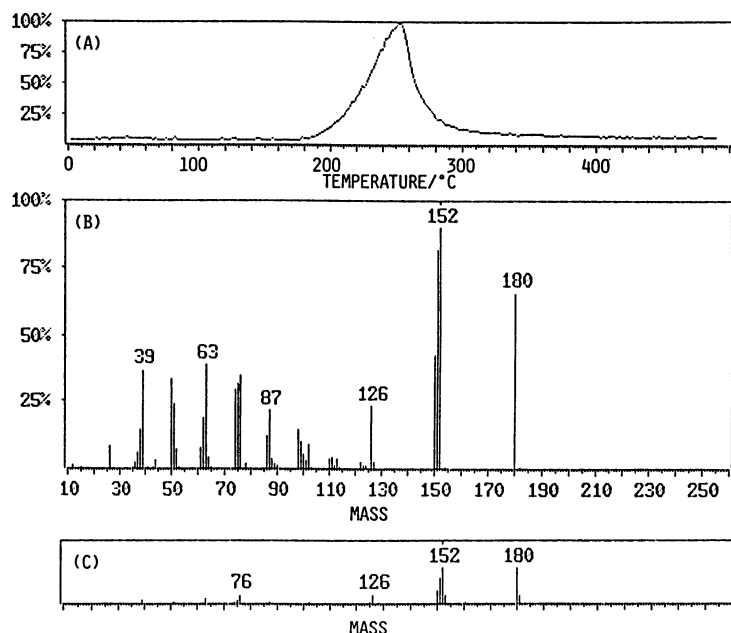
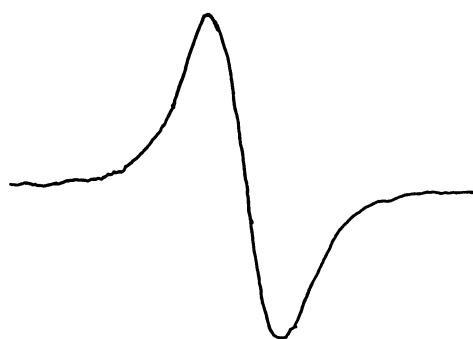


Fig. 7. DSC and TG curves of the Bc₂DDQ crystal.

Fig. 8. GC/MS spectra of the Bc₂DDQ crystal.

G VALUE = 2.0005 : ISOTROPIC VALUES
LINE WIDTH = 2.0 GAUSS

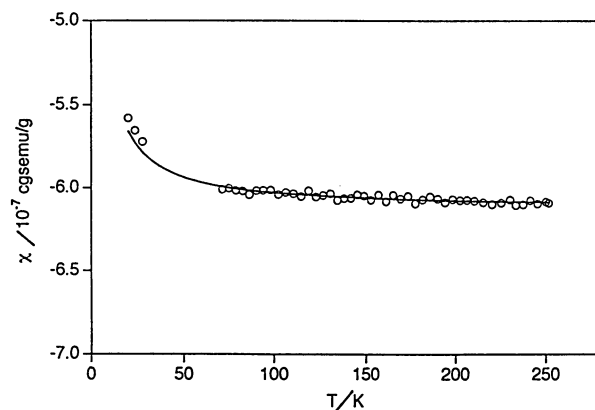
Fig. 9. ESR spectrum for the black product obtained by heating the Bc₂DDQ crystal.

Fig. 10. Temperature dependence of the magnetic susceptibility of the black product. A Curie fit was made for data above 80 K reproducing data below 30 K.

heating at 160 °C for 40 h is shown in Fig. 6-(2). Although the spectrum is very complicated, the peak at 2250 cm⁻¹ can be assigned to the C≡N stretching vibration, which is hardly observable in quinone; but strong in the semiquinone radical.⁹⁾ The C=O stretching vibration in quinone at 1695 cm⁻¹ for the Bc₂DDQ crystal before heating shifts to 1620 cm⁻¹ in semiquinone after heating. The change in the pattern in the region between 1500 and 700 cm⁻¹ is also remarkable.

The above-mentioned results show that the solid-phase reaction of Bc₂DDQ at about 150 °C is a polymerization reaction. Osawa et al. reported a dimerization reaction of *p*-benzoquinone via an intermediate of the CT complex between Wurster's Blue and *p*-benzoquinones in acetone.¹⁾ The present solid-phase reaction seems to be similar to their solution-phase

reaction.

Magnetic Properties of the Black Product. Figure 9 shows the ESR spectrum of the black pyroproduct. The ESR spectrum obtained at room temperature has the characteristic of the isotropic *g* value (*g*=2.0005) and the line width (2.0 Gauss, 1 Gauss=10⁻⁴ T). This fact means that the black product contains many stable radicals as bonding defects of the polymerization process. The concentration of radicals was estimated by measuring the temperature dependence of the magnetic susceptibility, as is shown in Fig. 10. The solid line is the best-fitted curve calculated by

$$\chi(T) = \chi_0 + \frac{C}{T}, \quad (6)$$

where $\chi_0 = -6.1 \times 10^{-7}$ cgs emu g⁻¹ and $C = 9.3 \times 10^{-7}$ cgs ems K g⁻¹.

Parameter C is expressed by

$$C = \frac{n}{M} \frac{N_A \beta^2}{3k} g^2 s(s+1) \\ = 0.125 \times \frac{n}{M} g^2 s(s+1). \quad (7)$$

Here, N_A is Avogadro's number, M the molecular weight of the Bc₂DDQ complex and n the spin number per Bc₂DDQ complex. Then, $M = 587.4$ g mol⁻¹, $g = 2.0005$, and $s = 1/2$ give a spin number of $n = 1.5 \times 10^{-3}$ per Bc₂DDQ complex.

The authors thank the Instrument center, Institute for Molecular Science, for the use of the Oxford magnetic balance. They also thank Mr. K. Mogi for carrying out the calculation using the Gaussian-90 program¹⁰⁾ on the FACOM M782 computers at the Nagoya University Computational Center.

References

- 1) K. Kanematsu, S. Morita, S. Fukushima, and E. Osawa, *J. Am. Chem. Soc.*, **103**, 5211 (1981).
- 2) Y. Osawa, N. Nishimura, and S. Yamamoto, *Bull. Chem. Soc. Jpn.*, **64**, 2648 (1991).
- 3) M. Tanaka, "4-th Jikken Kagakukouza," ed by K. Yoshihara, Maruzen, Vol. 4, Bunkou II, p. 314 (1992).
- 4) D. N. Vries Reilinsch and R. P. H. Rettschrick, *J. Chem. Phys.*, **54**, 2722 (1971).
- 5) A. Kuboyama, Y. Kozima, and J. Maeda, *Bull. Chem. Soc. Jpn.*, **55**, 3635 (1982).
- 6) B. Shaanan, U. Shmueli, and M. Colapietro, *Acta Crystallogr., Sect. B*, **38**, 818 (1982).
- 7) M. Tanaka, *Bull. Chem. Soc. Jpn.*, **50**, 2881 (1977).
- 8) M. Tanaka, *Bull. Chem. Soc. Jpn.*, **51**, 1001 (1978).
- 9) Y. Matsunaga, *J. Chem. Phys.*, **41**, 1609 (1964).
- 10) M. J. Frisch, M. Head-Gordon, G. W. Trucks, J. B. Foresman, H. B. Schlegel, K. Raghavachari, M. A. Robb, J. S. Binkley, C. F. Gonzalez, D. J. Defrees, D. J. Fox, R. A. Whiteside, R. Seeger, C. F. Melius, J. Baker, R. L. Martin, L. R. Kahn, J. J. P. Stewart, S. Topiol, and J. A. Pople, Gaussian, Inc., Pittsburgh PA 15213, (1990).